Propagators in Coulomb gauge from SU(2) lattice gauge theory

Kurt Langfeld and Laurent Moyaerts

Insitut für Theoretische Physik, Universität Tübingen, D-72076 Tübingen, Germany.
(Received 29 June 2004; published 13 October 2004)

A thorough study of 4-dimensional SU(2) Yang-Mills theory in Coulomb gauge is performed using large scale lattice simulations. The (equal-time) transverse gluon propagator, the ghost form factor $d(p)$ and the Coulomb potential $V_{\text{coul}}(p) \propto d^2(p)f(p)/p^2$ are calculated. For large momenta p, the gluon propagator decreases like $1/p^{1+\eta}$ with $\eta = 0.5(1)$. At low momentum, the propagator is weakly momentum dependent. The small momentum behavior of the Coulomb potential is consistent with linear confinement. We find that the inequality $\sigma_{\text{coul}} \geq \sigma$ is satisfied. Finally, we provide evidence that the ghost form factors $d(p)$ and $f(p)$ acquire IR singularities, i.e., $d(p) \propto 1/\sqrt{p}$ and $f(p) \propto 1/p$, respectively. It turns out that the combination $g_0^2 d_0(p)$ of the bare gauge coupling g_0 and the bare ghost form factor $d_0(p)$ is finite and therefore renormalization group invariant.

I. INTRODUCTION

Quark confinement is the key property which dictates the structure of matter at low temperatures and densities. It is attributed to the low-energy regime of Quantum Chromo Dynamics (QCD) and is, therefore, only accessible by nonperturbative techniques. Lattice gauge theory provides a gauge invariant regularization of Yang-Mills theory, and corresponding numerical simulations do not require gauge fixing.

More than 20 years ago, Mandelstam and G.'t Hooft pointed out that gauge fixing might be convenient for identifying the degrees of freedom which are relevant for confinement. Over the recent past, evidence has been accumulated by means of lattice simulations that topological obstructions of the gauge field, such as monopoles and vortices, are responsible for confinement (see [1] for a recent review). Nonperturbative approaches based on Dyson-Schwinger equations (DSE) [2,3], variational techniques [4–6] and flow equations [7,8] necessarily involve gauge fixing. These approaches address QCD Green functions which encode information on confinement at low momenta.

In Landau gauge, it was firstly put forward by Gribov [9] and further elaborated by Zwanziger [10] that quark confinement is associated with a divergence of the ghost form factor in the infrared limit. First indications that the so-called horizon criterion for confinement is satisfied were reported in [11]. Using truncated DSEs, strong evidence for an IR divergent ghost form factor was reported in [12,13]. Subsequently, many efforts were devoted to detect the low-energy behavior of the ghost form factor by means of analytic [14–19] and lattice [20–22] techniques. A good qualitative agreement between the DSE and lattice results was found. Moreover, a tight relation between the vortex picture of confinement and the Gribov-Zwanziger criterion was given in [23].

Coulomb gauge is most convenient for a variational approach to Yang-Mills Green functions [4–6]. The cor-responding Hamiltonian contains an instantaneous interaction between color sources, the so-called Coulomb potential $V_{\text{coul}}(r)$. Hence, Coulomb gauge QCD offers the possibility to address the confining potential by purely analytic considerations. It has been shown recently [24] that the Coulomb potential is an upper bound of the static quark-antiquark potential. In pure Yang-Mills theory, both potentials are expected to be linearly rising at large distances r, i.e., $V = \sigma r$ and $V_{\text{coul}} = \sigma_{\text{coul}} r$, where (σ_{coul}) σ is called (Coulomb) string tension. At present, lattice simulations provide two different values for the asymptotic Coulomb force: A calculation of the potential involving the zeroth component of the gauge field yields $\sigma_{\text{coul}} \approx (2-3)\sigma$ [25,26], while $\sigma_{\text{coul}} \approx \sigma$ [27] is reported if the Green function which defines the Coulomb potential is directly evaluated.

The variational approach invokes a quasiparticle picture for the (transverse) gluons. The trial wave functional generically is Gaussian, and the gluon dynamics is encoded in the (quasiparticle) gap function ω_{QP} (which is derived in a gluonic quasiparticle picture from the inverse of the instantaneous gluon propagator). It was recently proposed to supplement the Faddeev-Popov determinant (see below) to the wave functional in order to strengthen the impact of configurations close to the Gribov horizon [6]. The latter modification of the wave functional has certainly a strong impact on the gap function at least at small momenta: while it is suggested in [4] that ω_{QP} approaches a constant in the IR limit, an IR divergence was reported in [6]. Both approaches employ a truncation of the resulting Dyson equations which does not account for wave functional renormalization.

In the present paper, we perform a thorough lattice investigation of the transverse gluon propagator, the ghost form factor and the Coulomb potential. Our results suggest that (at least in four dimensions) the equal-time gluon propagator is weakly momentum dependent in the IR regime. For the first time, wave-function renormal-

70 074507-1

ization constants for the gluon and ghost fields are obtained. Our lattice results indicate quite a sizable anomalous dimension for the gluon propagator yielding $G(|\mathbf{p}|) \rightarrow 1/|\mathbf{p}|^{1+\eta}$ where $\eta \approx 0.5$. Our results for the Coulomb potential are compatible with linear confinement and suggest that the inequality $\sigma_{\text{coul}} \gtrsim \sigma$ is satisfied. We will find that the result $\sigma_{\text{coul}} \approx (2-3)\sigma$, reported in [25,26], cannot be ruled out by our data.

II. THE PARTITION FUNCTION

Let us briefly review the relation between the functional integral formulation and the Hamilton formulation of Coulomb gauge Yang-Mills theory following [28]. Our starting point will be the generating functional for Euclidean Green functions in Coulomb gauge, i.e.,

$$Z[J] = \int \mathcal{D}A \exp\left\{\int \mathcal{L}d^4x\right\}\delta(\partial_i A_a^i)\text{Det}[-\nabla \cdot \mathbf{D}],$$
$$\mathcal{L} = -\frac{1}{4}F_{\mu\nu}^a F_a^{\mu\nu} - ig_0 A_\mu^a J_a^\mu, \tag{1}$$

where A_μ^a are the gauge fields, $F_{\mu\nu}^a$ denotes the usual field strength tensor and J_a^μ is an external source. $\text{Det}[-\nabla \cdot \mathbf{D}]$ is the Faddeev-Popov determinant (**D** is the gauge covariant derivative), and g_0 the bare gauge coupling. Equation (1) will serve as the starting point for the lattice simulations reported in this work.

The canonical momenta conjugated to the gauge fields are introduced by

$$\int \mathcal{D}\mathbf{\Pi} \exp\left\{-\int d^4x\left(\frac{1}{2}\mathbf{\Pi}^2 - i\Pi_i^a F_a^{0i}\right)\right\} = \exp\left\{-\frac{1}{2}\int d^4x F_{0i}^a F_a^{0i}\right\}.$$

Eliminating the nondynamical part of the gauge fields, A_0^a, implements Gauss's law in the partition function, i.e.,

$$Z = \int \mathcal{D}\mathbf{A}\mathcal{D}\mathbf{\Pi} \exp\left\{\int d^4x\left[i\Pi_i^a \dot{A}^{i,a} - \frac{1}{2}(\mathbf{\Pi}^2 + \mathbf{B}^2)\right.\right.$$
$$\left.\left. - g_0\mathbf{A}^a \cdot \mathbf{J}^a\right]\right\}\delta(\partial_i A_i^a)\delta([D_i\Pi^i]^a - g_0 J_0^a)$$
$$\times \text{Det}[-\nabla \cdot \mathbf{D}]. \tag{2}$$

In this expression, **B** denotes the chromo-magnetic field $B_k^a = -\frac{1}{2}\varepsilon_{ijk}F_{ij}^a$. Let us introduce the transverse and longitudinal parts of the canonical momenta by $\mathbf{\Pi}^a = \mathbf{\Pi}_\perp^a - \nabla\phi^a$. The integration measure factorizes, i.e., $\mathcal{D}\mathbf{\Pi} \simeq \mathcal{D}\mathbf{\Pi}_\perp \mathcal{D}\phi$, and the integration over ϕ cancels the Faddeev-Popov determinant. One finally obtains

$$Z = \int \mathcal{D}\mathbf{A}_\perp \mathcal{D}\mathbf{\Pi}_\perp \exp\left\{\int d^4x(i\Pi_{\perp,i}^a \dot{A}^{i,a} - \mathcal{H}_\perp)\right\}. \tag{3}$$

The Hamiltonian density $\mathcal{H}_\perp$ gives rise to the Coulomb gauge Hamiltonian $H = \int d^3x \mathcal{H}_\perp$:

$$H = \int d^3x\left[\frac{1}{2}(\mathbf{\Pi}_\perp^2 + \mathbf{B}^2) + g_0\mathbf{A}_\perp \cdot \mathbf{J}\right] - \frac{1}{2C_2}$$
$$\times \int d^3x d^3y \rho(t, \mathbf{x})\mathcal{V}_{\text{Coul}}(\mathbf{x}, \mathbf{y})\rho(t, \mathbf{y}), \tag{4}$$

where C_2 is the quadratic Casimir of the gauge group SU(2), i.e., $C_2 = 3/4$. We have introduced the color charge density by [$x = (t, \mathbf{x})$]

$$\rho(x) = f^{abc}A_i^b(x)\Pi_{\perp i}^c(x) + J_0(x). \tag{5}$$

The "tree level" term which mediates the interaction between color charges, i.e.,

$$\mathcal{V}_{\text{Coul}}(\mathbf{x}, \mathbf{y}) = -C_2 g_0^2 M^{-1}(-\Delta)M^{-1}|_{(\mathbf{x},\mathbf{y})}, \tag{6}$$

where Δ denotes the Laplace operator, will give rise to the so-called Coulomb potential upon averaging over the gauge fields. Thereby,

$$M = -\nabla \cdot \mathbf{D} \tag{7}$$

is the Faddeev-Popov matrix.

III. THE NUMERICAL APPROACH

A. Setup

Configurations of a N^4 cubic lattice with lattice spacing a are generated using the standard Wilson action. A lattice configuration is represented by a set of unitary matrices $U_\mu(x) \in$ SU(2). The size of the lattice spacing as a function of the Wilson β parameter is obtained from the interpolating formula [22]

$$\ln(\sigma a^2) = -\frac{4\pi^2}{\beta_0}\beta + \frac{2\beta_1}{\beta_0^2}\ln\left(\frac{4\pi^2}{\beta_0}\beta\right) + \frac{4\pi^2}{\beta_0}\frac{d}{\beta} + c, \tag{8}$$

where

$$\beta_0 = \frac{22}{3}, \qquad \beta_1 = \frac{68}{3}. \tag{9}$$

The first two terms on the r.h.s. of (8) are in accordance with 2-loop perturbation theory. The term d/β represents higher-order effects and the term c is a dimensionless scale factor to the string tension. It was observed [22] that the choice

$$c = 4.38(9), \qquad d = 1.66(4) \tag{10}$$

reproduces the measured value σa^2 to very good precision.

Two possible definitions of the gauge field $A_\mu^b(x)$ in terms of the link matrices are explored in the present paper. Decomposing a particular SU(2) matrix by

$$U_\mu(x) = u_\mu^0(x) + iu_\mu^a(x)\tau^a, \tag{11}$$

where τ^a are the Pauli matrices, the standard definition of the gauge field is given by

$$ag_0 A_\mu^b(x) + \mathcal{O}(a^3) = 2u_\mu^b(x). \tag{12}$$

Noticing that the continuum gauge fields actually transform under the adjoint representation, the definition

$$ag_0 A_\mu^b(x) + \mathcal{O}(a^3) = 2u_\mu^0(x)u_\mu^b(x) \tag{13}$$

accounts for this particular transformation property [29]. Note that both definitions coincide in the continuum limit $a \to 0$. In the context of minimal Landau gauge, both definitions also coincided at the practical level within the scaling window [22].

Finally, we define the momentum on the lattice for the particular direction μ

$$p_\mu := \frac{2}{a}\sin(\frac{\pi}{N}n_\mu), \tag{14}$$

where $-N/2 < n_\mu \leq N/2$ labels the Matsubara frequency. This definition minimizes rotational symmetry breaking for momenta close to the boundary of the Brillouin zone.

B. Propagators and Coulomb potential

Once and for all, we choose a given time slice of the four dimensional space-time by fixing $t = t_0$, and consider propagators which are defined within the emerging 3-dimensional hypercube.

The unrenormalized gluon propagator is defined by

$$G_{ij}^{0ab}(\mathbf{x} - \mathbf{y}) := \langle A_i^a(\mathbf{x}, t_0) A_j^b(\mathbf{y}, t_0) \rangle. \tag{15}$$

The corresponding propagator in momentum space, i.e.,

$$G_{ij}^{0ab}(\mathbf{p}) = \int d^3x \, G_{ij}^{0ab}(\mathbf{x}) e^{i\mathbf{p}\cdot\mathbf{x}},$$

is transversal by virtue of the gauge condition $\partial_i A_a^i(\mathbf{x}, t_0) = 0$ and diagonal in color space, i.e.,

$$G_{ij}^{0ab}(\mathbf{p}) = \left(\delta_{ij} - \frac{p_i p_j}{\mathbf{p}^2}\right)\delta^{ab}G^0(\mathbf{p}), \tag{16}$$

$$G^0(\mathbf{p}) = \frac{f_g^0(\mathbf{p})}{|\mathbf{p}|}. \tag{17}$$

The dimensionless quantity f_g^0 is the (bare) gluon form factor. Since the gauge potential has energy dimension one, the quantity $G^0(\mathbf{p})$ has the dimension of an inverse energy.

The (bare) ghost propagator is defined as the expectation value of the inverse Faddeev-Popov operator M in (7), i.e.,

$$D^{0ab}(\mathbf{x} - \mathbf{y}) = \langle M^{-1}[A]|_{(\mathbf{x},\mathbf{y})}^{ab} \rangle. \tag{18}$$

Since D^{ab} is diagonal in color space, we may write

$$D^{0ab}(\mathbf{p}) = \delta^{ab}D^0(\mathbf{p}), \qquad D^0(\mathbf{p}) = \frac{d^0(\mathbf{p})}{|\mathbf{p}|^2}$$

in momentum space. Thereby, we have introduced the (bare) *ghost form factor* $d^0(\mathbf{p})$. Since the quantity $\langle M^{-1}[A]|_{(\mathbf{x},\mathbf{y})} \rangle$ has energy dimension 1, the ghost form factor $d^0(\mathbf{p})$ is dimensionless and reduces to unity for a free theory.

The Coulomb potential is given by the expectation value of the expression (6):

$$V_{\text{Coul}}^0(\mathbf{x} - \mathbf{y})\delta^{ab} = -C_2 g_0^2 \langle \{M^{-1}[A](-\Delta)M^{-1}[A]\} \rangle. \tag{19}$$

For the Fourier transform of the Coulomb potential, we make the ansatz

$$V_{\text{Coul}}^0(\mathbf{p}) = -C_2 g_0^2 \frac{d_0^2(\mathbf{p})f(\mathbf{p})}{|\mathbf{p}|^2}, \tag{20}$$

where $d^0(\mathbf{p})$ is the bare ghost form factor. The dimensionless function $f(\mathbf{p})$ measures the deviation from the factorization

$$\langle M^{-1}[A](-\Delta)M^{-1}[A] \rangle = \langle M^{-1}[A] \rangle(-\Delta)\langle M^{-1}[A] \rangle, \tag{21}$$

in which case $f(\mathbf{p}) = 1$.

C. Renormalization

Renormalization of Yang-Mills theories in four dimensions implies that the bare coupling acquires a dependence on the ultraviolet (UV) cutoff Λ_{UV}, i.e.,

$$g_0 \to g_0(\Lambda_{\text{UV}}/\Lambda_{\text{QCD}}). \tag{22}$$

Rather than the bare coupling constant, the Yang-Mills scale parameter Λ_{QCD} plays the role of the only parameter of the theory. In the context of (quenched) lattice gauge simulations the string tension σ is widely used as the generic low-energy scale. In this case, the cutoff dependence of the bare coupling is implicitly given by the β dependence of $\sigma a^2(\beta)$ where $\beta = 4/g_0^2$ is related to the cutoff by $\Lambda_{\text{UV}} = \pi/a(\beta)$. Finally, the relation between σa^2 and β is provided by the formula (8) which interpolates the calculated values.

In addition, wave-function renormalization constants generically develop a dependence on $\Lambda_{\text{UV}}/\Lambda_{\text{QCD}}$. The lattice bare form factors of the previous subsections, f_g^0 and d^0, depend on the momentum p^2 and on the UV cutoff Λ_{UV} (given in units of the string tension) or, equivalently, on the lattice coupling β. The renormalized form factors are obtained upon multiplicative renormalization

$$f_g^{\text{ren}}(p^2, \mu^2) = Z_3^{-1}(\beta, \mu)f_g^0(p^2, \beta), \tag{23}$$

$$d^{\text{ren}}(p^2, \mu^2) = \tilde{Z}_3^{-1}(\beta, \mu)d^0(p^2, \beta), \tag{24}$$

using the renormalization conditions

$$f_g^{\text{ren}}(\mu^2, \mu^2) = 1, \qquad d^{\text{ren}}(\mu^2, \mu^2) = 1. \qquad (25)$$

Finally note that the Coulomb potential $V_{\text{Coul}}(\mathbf{p})$ (20) appears as a convolution of propagators. Let us factor out the wave-function renormalization of the ghost fields, and let us introduce the renormalization constant Z_f of the 4-point vertex function involving four ghost fields:

$$V_{\text{Coul}}^{\text{ren}}(\mathbf{p}, \mu^2) = Z_f^{-1}(\beta, \mu)\widetilde{Z}_3^{-2}(\beta, \mu)V_{\text{Coul}}^0(\mathbf{p}, \beta), \quad (26)$$

where V_{Coul}^0 is given in (19). If the theory is renormalizable without a 4-ghost counter term at tree level, then

$$\lim_{\beta \to \infty} Z_f(\beta, \mu) = \text{constant}, \qquad (27)$$

and the "factorization" function $f(\mathbf{p})$, which is implicitly defined by (20), does not acquire an UV divergence. Since a 4-ghost interaction is a marginal relevant term, it cannot be excluded from the action by first principles. We will find, however, that the lattice approach can be consistently treated without such a counter term. Below, we will suppress the superscript "ren" and only deal with renormalized quantities.

Multiplicative renormalizability of the theory implies that a rescaling of the data for each β value (independently of the momentum) is sufficient to let the form factors fall on top of a single curve describing the momentum dependence of the corresponding renormalized quantity. In practice, suitable "matching factors" are determined which "collapse" data obtained at different β on a single curve. The matching factors are then directly related to the wave-function renormalization constants. This procedure is described in detail in [30], Sec. V.B.2, and [22].

D. Gauge fixing

Let us consider the time slice t_0 in which we define the transverse (equal-time) gluon propagator (15) and the ghost propagator, respectively.

The lattice configurations are generated without any preference for a particular gauge. Subsequently, the gauge transformations $\Omega(x)$ are adjusted according to

$$F_U[\Omega] = \sum_{\vec{x}, i=1...3} \text{ReTr}[1 - U_i^\Omega(\vec{x}, t_0)] \overset{\Omega}{\to} \text{min}, \qquad (28)$$

where

$$U_\mu^\Omega(x) = \Omega(x)U_\mu(x)\Omega^\dagger(x + \mu).$$

It is well known that the condition (28) fixes the gauge up to gauge transformations which only depend on time, i.e., $\Omega(t)$. Note, however, that the average over the unfixed gauge degree of freedom does not affect the (equal-time) gluon propagator. The same is true for the ghost propagator.

The calculation of the noninstantaneous generalized gluon propagator, i.e.,

$$G_{ij}^{\text{gen}ab}(\mathbf{x} - \mathbf{y}, t - t_0) := \langle A_i^a(\mathbf{x}, t)A_j^b(\mathbf{y}, t_0) \rangle, \qquad (29)$$

would inevitably require complete gauge fixing, since the residual gauge freedom would imply

$$G_{ij}^{\text{gen}ab}(\mathbf{x} - \mathbf{y}, t - t_0) = 0 \quad \text{for } t \neq t_0.$$

The standard procedure is to involve the gauge field $A_0^a(x)$ for residual gauge fixing. An example is the Cucchieri-Zwanziger condition [31]

$$F_t[\Omega] = \sum_{\vec{x}, t} \text{ReTr}[1 - U_0^\Omega(\vec{x}, t)] \overset{\Omega(t)}{\to} \text{min}. \qquad (30)$$

It is also possible to fix the residual gauge freedom without incorporating $A_0^a(x)$. In this case, the $A_0^a(x)$ integration in Sec. II can still be performed, thereby enforcing Gauss's law (see (2)). The advantage is that the tight relation between the functional approach (1) and the Hamiltonian formulation (3) is preserved.

After averaging over the gauge fields, the Fourier transform of (29) can be written as

$$G_{ij}^{\text{gen}ab}(\mathbf{p}, p_0) = \delta^{ab}\left(\delta_{ij} - \frac{p_i p_j}{\mathbf{p}^2}\right)\frac{F(\mathbf{p}, p_0)}{\mathbf{p}^2}, \qquad (31)$$

where the dimensionless quantity $F(\mathbf{p}, p_0)$ is a form factor. If the residual gauge degree of freedom is not fixed, the gauge fields corresponding to different time slices would be uncorrelated, and the form factor would not depend on p_0. We expect that the residual gauge fixing only introduces weak correlations between gauge fields of different time slices implying that the form factor only slightly depends on p_0. A detailed lattice investigation is left to the near future. In the present paper, we will focus on the equal-time gluon propagator (15).

In practice, we used a *simulated annealing* method to locate the minimum of (28). The idea is to consider the gauge functional $F_U[\Omega]$ as the action of a field theory with respect to the set of the gauge transformations $\Omega(\mathbf{x})$, whose partition function is given by

$$Z_{\text{SA}} = \int D\Omega \exp(-\beta_{\text{SA}}F_U[\Omega]).$$

By increasing step by step the free parameter β_{SA} (which plays the role of the inverse temperature), one tries by cooling to retrieve the ground state of the fictitious field theory. This procedure corresponds to the minimization of $F_U[g]$. The thermalization steps can be performed using the standard Creutz update algorithm supplemented by microcanonical reflection steps. After the domain of attraction has been located by simulated annealing, we perform *iterated overrelaxation* to ensure the desired precision of the gauge condition. Details will be presented elsewhere. At least in minimal Landau gauge, it has turned out that the present method of gauge fixing is robust against the impact of Gribov ambiguities [22].
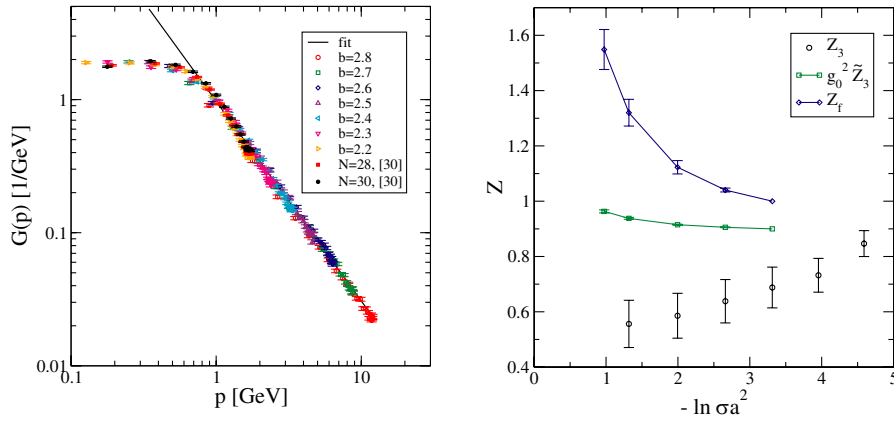
FIG. 1 (color online). The transverse equal-time gluon propagator as a function of the momentum: our data ($N = 42$) and data from [31] (left panel). The gluon wave-function renormalization constant Z_3 as a function of the UV cutoff. Also shown are the wave functional renormalization constant of $g_0^2 d(\mathbf{p})$ and Z_f (26); the y-axis is arbitrarily scaled (right panel).

IV. NUMERICAL RESULTS

A. Gluon propagator

Lattice simulations were carried out using 26^4, 32^4 and 42^4 lattices. Inverse couplings $\beta \in \{2.2, 2.3, 2.4, 2.5, 2.6, 2.7, 2.8\}$ were employed. Within the momentum window, very good scaling is observed implying that cutoff effects (due to the finite value a) and finite size effects are small. Our final result for the transverse equal-time gluon propagator $G(\mathbf{p})$ (17) is shown in Fig. 1. Only data for the 42^4 lattice are shown for clarity. We have checked that the data for the 26^4, 32^4 lattices fall on top of the same curve. As a renormalization condition, we have chosen

$$G(\mathbf{p} = 1\text{GeV}) = 1[\text{GeV}]^{-1} \qquad (32)$$

for a renormalization point $\mu = 1$ GeV. For comparison, we have also shown the data obtained by Cucchieri and Zwanziger in [31]. These data are obtained for $\beta = 2.2$ and 28^4, 30^4 lattices by using an iterated overrelaxation method for gauge fixing. We find good agreement.

At small momentum, the propagator becomes roughly momentum independent and seems to approach a constant in the IR limit $|\mathbf{p}| \to 0$. At large momentum, the momentum dependence is well approximated by

$$G(\mathbf{p}) \propto \frac{1}{|\mathbf{p}|}\left(\frac{\Lambda_{\text{QCD}}}{|\mathbf{p}|}\right)^{\eta}, \qquad \eta = 0.5(1), \qquad (33)$$

where Λ_{QCD} is the renormalization group invariant scale parameter. The solid line in Fig. 1 corresponds to a fit with $\eta = 0.5$. The large value η was already anticipated in [31]. Since the authors focused their investigations on the IR behavior of the gluon propagator, they concluded that their data, obtained for momenta below 2 GeV, did not reach the perturbative regime. In the present paper, the high momentum regime is also explored. It turns out that the trend with η as large as 0.5 continues at least up to momenta as large as 12 GeV.

Also shown in Fig. 1 is the cutoff dependence of the wave-function renormalization constant Z_3. Unfortunately, the achieved numerical precision does not allow
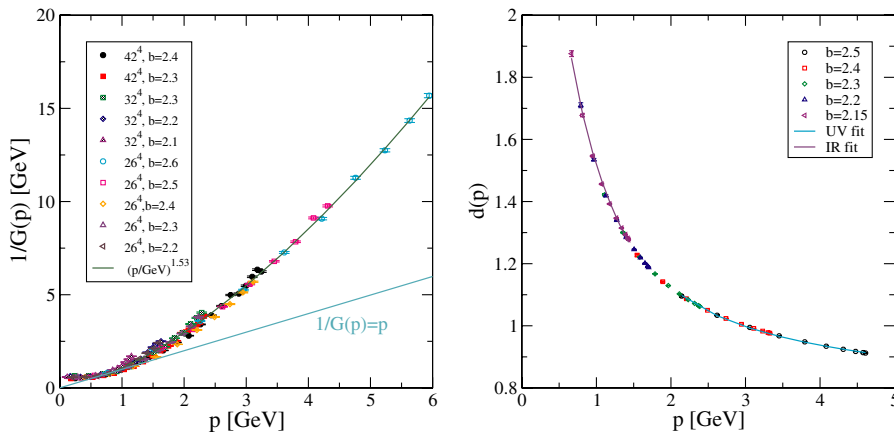

FIG. 2 (color online). Momentum dependence of the inverse gluon propagator $1/G(\mathbf{p})$ (left panel). Ghost form factor (right panel).

for a definite conclusion on the functional form which parameterizes the cutoff dependence of Z_3.

In the context of a variational approach [4–6], $1/G(\mathbf{p})$ is interpreted as energy dispersion relation of constituent gluon fields. Note, however, that the full gluon propagator $G(\mathbf{p})$ which comprises all nonperturbative effects is parameterized by $G(\mathbf{p}) = g(\mathbf{p})/\omega_{QP}(\mathbf{p})$, where $g(\mathbf{p})$ accounts for effects which are beyond the leading order of the quasiparticle (QP) picture. Hence, the interpretation of the inverse propagator as dispersion relation must be taken with care. Our results for the inverse gluon propagator $1/G(\mathbf{p})$ for several lattice sizes are shown in Fig. 2.

B. Ghost form factor

In order to obtain the ghost propagator (18), an inversion of the Faddeev-Popov matrix is performed after (possible) zero modes have been removed [11]. This procedure requires the solution of large, but sparse, systems of equations. In order to remove zero mode contributions, we solve

$$MMx = Mb,$$

rather than the system $Mx = b$ (see the method proposed in [11]). For this purpose, we use the minres algorithm with Jacobi preconditioning [32]. Our final result for the ghost form factor $d(\mathbf{p})$ obtained from simulations using a 26^4 lattice and $\beta \in \{2.15, 2.2, 2.3, 2.4, 2.5\}$ is shown in Fig. 2, right panel. We observe perfect scaling. To be specific, we choose

$$d(\mathbf{p} = 3 \text{ GeV}) = 1$$

as a renormalization condition.

In order to explore the high momentum dependence, we make a logarithmic ansatz supplemented with an anomalous dimension γ_g, i.e.,

$$d(\mathbf{p}) = \frac{a_{uv}}{\ln(|\mathbf{p}|/\Lambda_{QCD})^{\gamma_{go}}}, \qquad p \gg \Lambda_{QCD}. \qquad (34)$$

The UV fit shown in Fig. 2 (right panel) corresponds to

$$a_{uv} \approx 1.03(2), \qquad \gamma_{go} = 0.26(2).$$

Since the fitting parameters are strongly correlated, it is difficult to extract a reliable value for Λ_{QCD}. Taking also into account the high momentum behavior of the Coulomb potential (see below), we find that

$$\Lambda_{QCD} = 0.96(5) \text{ GeV}$$

reproduces the UV data. Such a high value for the Yang-Mills scale parameter seems to be generic for the lattice regularization (see [22,33]). For the IR analysis, we adopt a simple scaling law:

$$d(\mathbf{p}) = \frac{a_{ir}}{(|\mathbf{p}|^2/\Lambda_{QCD}^2)^\kappa}, \qquad p \ll \Lambda_{QCD}. \qquad (35)$$

The IR fit is also shown in Fig. 2 (right panel). We find

$$a_{ir} \approx 1.55(1), \qquad \kappa = 0.245(5). \qquad (36)$$

Hence, our lattice results suggest that the ghost form factor roughly diverges like $1/\sqrt{|\mathbf{p}|}$ in the IR limit $|\mathbf{p}| \to 0$.

Let us explore the ghost wave-function renormalization constant $\tilde{Z}_3$. If one applies the momentum matching technique to $g_0^2 d_0(\mathbf{p}, \beta)$, one finds that the matching factors are constant within the numerical precision, see Fig. 1, right panel. Our findings therefore suggest that the bare coupling squared times the bare ghost propagator, i.e.,

$$g_0^2 D_0^{ab}(\mathbf{p}), \qquad (37)$$

is a renormalization group invariant.

C. Coulomb potential

In the present approach, the Coulomb potential appears as a convolution of Green functions (see (19)). In full Yang-Mills theory, wave functional (and vertex) renormalization applies (see (26)), and the prefactor of the potential must be specified by a renormalization condition. The prefactor can be determined by demanding that the perturbative result is recovered [28] at large momentum, i.e.,

$$\mathbf{p}^2 V_{\text{Coul}}(\mathbf{p}) \approx \frac{6\pi}{11 \ln|\mathbf{p}|^2/\Lambda_{QCD}^2}, \qquad (38)$$

for $|\mathbf{p}| \gg \Lambda_{QCD}$. An elegant method which circumvents the cumbersome determination of the prefactor was put forward in [25,26].

Our numerical findings for $p^2 V_{\text{Coul}}(\mathbf{p})$ are summarized in Fig. 3 (left panel). At large momentum, the lattice data nicely show the logarithmic correction. The data of low-energy regime are well reproduced by the scaling ansatz

$$\mathbf{p}^2 V_{\text{Coul}}(\mathbf{p}) \approx \frac{c}{(|\mathbf{p}|^2/\Lambda_{QCD}^2)^\delta}, \qquad (39)$$

where c is related to the Coulomb string tension σ_{Coul} by $\sigma_{\text{Coul}} = c\Lambda_{QCD}^2/8\pi$ in case V_{Coul} is compatible with linear confinement ($\delta = 1$). Here, we find (see Fig. 3, left panel)

$$\delta = 1.05(5), \qquad c = 4.9(2). \qquad (40)$$

Also shown in Fig. 3 (right panel) is the combination

$$\mathbf{p}^4 V_{\text{Coul}}(\mathbf{p})/8\pi\sigma,$$

which should approach $\sigma_{\text{coul}}/\sigma$ in the limit $|\mathbf{p}| \to 0$. Already for $p > 2$ GeV, the perturbative result is recovered to good precision. A plateau is reached at the intermediate momentum range $1\text{GeV} < p < 2\text{GeV}$. The function is slightly increasing again for $p < 1\text{GeV}$. The data within the observed momentum window are stable against finite size effects. An extrapolation $p \to 0$ is cumbersome. We point out that values $\sigma_{\text{coul}}/\sigma$ ranging from two to three reported in [25,26] cannot be ruled out
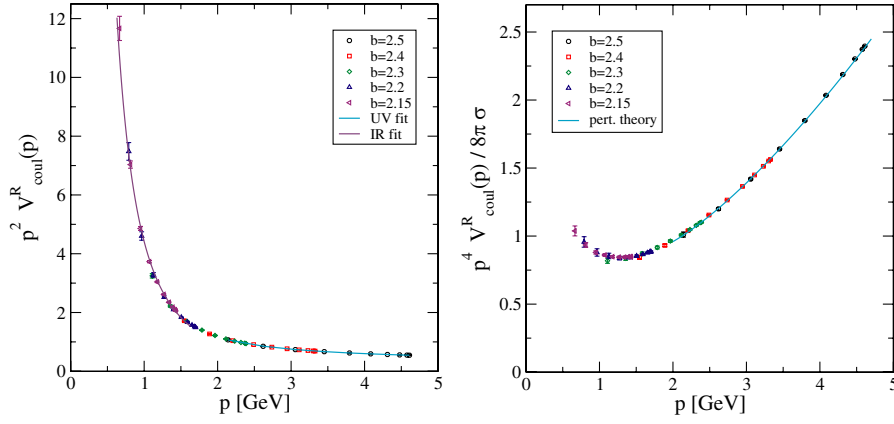
FIG. 3 (color online). $p^2 V_{\text{Coul}}(\mathbf{p})$ (Coulomb potential) as a function of the momentum $\mathbf{p}$ (left panel). $p^4 V_{\text{Coul}}(\mathbf{p})/8\pi$ in units of the string tension σ (right panel).

from the present data. Larger lattices and higher statistics will be necessary to explore the deep infrared regime.

D. Factorization

From the results of the previous subsections it is already clear that the function $f(\mathbf{p})$ cannot weakly depend on $|\mathbf{p}|$. Factorization such as (21) is generic if the fields are distributed according to a Gaussian probability distribution. Since the ghost fields are strongly interacting at low momenta, one expects that $f(\mathbf{p})$ significantly depends on the momentum in the IR regime.

In order to extract $f(\mathbf{p})$ from the lattice data we applied the following procedure: Dividing the bare data for $\mathbf{p}^2 V^0_{\text{coul}}$ with the bare ghost form factor squared provides information on the unrenormalized function $f^0(\mathbf{p})$. Applying the momentum matching technique [22] yields the renormalization constant Z_f and the renormalized function $f(\mathbf{p})$. Our numerical result for Z_f as a function of the UV cutoff is consistent with (see Fig. 1, right panel)

$$\lim_{\beta \to \infty} Z_f(\beta, \mu) = \text{constant}.$$

The function $f(\mathbf{p})$ is shown in Fig. 4. We observe a weak momentum dependence in the UV regime, and an IR singularity at small momentum. The high energy data are reproduced by the ansatz

$$f(\mathbf{p}) = \frac{a^f_{uv}}{\ln(|\mathbf{p}|/\Lambda_{\text{QCD}})^{\gamma_f}}, \qquad p \gg \Lambda_{\text{QCD}}. \quad (41)$$

The UV fit shown in Fig. 4 corresponds to

$$a^f_{uv} \approx 1.05(4), \qquad \gamma_f = 0.47(3).$$

The low momentum data support the existence of a $1/|\mathbf{p}|$ singularity, i.e.,

$$f(\mathbf{p}) = \frac{a^f_{ir}}{(|\mathbf{p}|^2/\Lambda^2_{\text{QCD}})^{\kappa_f}}, \qquad p < \Lambda_{\text{QCD}}, \quad (42)$$

with

$$a^f_{ir} \approx 2.7(1), \qquad \kappa_f = 0.58(5). \quad (43)$$

Our findings suggest the following interpretation: Due to asymptotic freedom, the expectation value on the left hand side of (21) factorizes in the high momentum regime. At low momentum, non-Gaussian correlations between the ghost fields play an important role and the factorization assumption is ruled out.

Finally, we point out that the sum rule, dictated by perturbation theory, i.e., $2\gamma_{go} + \gamma_f = 1$, is satisfied to good precision:

$$2\gamma_{go} + \gamma_f = 0.99(12). \quad (44)$$

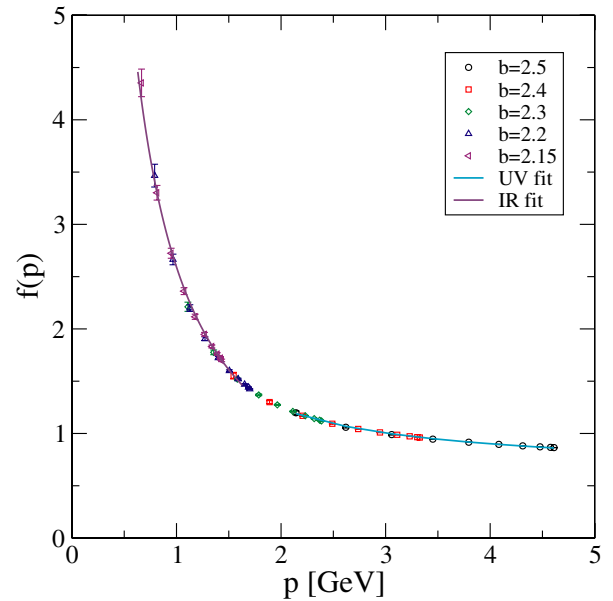This serves as a consistency check of the lattice renormalization procedure.

FIG. 4 (color online). The factorization function $f(\mathbf{p})$.

V. CRITICAL REMARKS

A. Equal-time gluon propagator

In Subsection IVA, the lattice data for the transverse equal-time gluon propagator $G(\mathbf{p})$ are consistent with the high momentum behavior $G(\mathbf{p}) \propto |\mathbf{p}|^{-1-\eta}$, $\eta = 0.5(1)$. It is tempting to conclude that asymptotic freedom implies the decrease of the equal-time gluon propagator $G(\mathbf{p})$ like $1/|\mathbf{p}|$ for large momenta. We stress that this conclusion does not necessarily apply: The equal-time gluon propagator $G(\mathbf{p})$ is derived from the generalized propagator (31) by momentum projection, i.e.,

$$G(\mathbf{p}) \propto Z_3^{-1} \int dp_0 G^{\mathrm{gen}}(\mathbf{p}, p_0) = Z_3^{-1} \int dp_0 \frac{F(\mathbf{p}, p_0)}{\mathbf{p}^2}. \tag{45}$$

After proper renormalization, the dimensionless form factor can be parameterized by

$$F(\mathbf{p}, p_0) = h\left(\frac{\Lambda_{\mathrm{QCD}}}{|\mathbf{p}|}, \frac{p_0}{|\mathbf{p}|}\right), \tag{46}$$

where Λ_{QCD} is the low-energy scale parameter (e.g., given by the string tension). For large momenta $|\mathbf{p}| \gg \Lambda_{\mathrm{QCD}}$, one obtains

$$G(\mathbf{p}) \approx Z_3^{-1} \frac{1}{|\mathbf{p}|} \int du \, h(0, u). \tag{47}$$

If the function $h(x, y)$ is completely regular and bounded for $x, y \in [0, \infty[$, the integral in the latter equation would exist implying that $G(\mathbf{p}) \propto \frac{1}{|\mathbf{p}|}$ for large $|\mathbf{p}|$. However, the form factor $F(\mathbf{p}, p_0)$ weakly depends on p_0 by the choice of the gauge (see discussions below (31)). Let us speculate that for this reason we might assume for $u \gg 1$ that

$$h(0, u) \propto \frac{1}{u^{1-\eta}} \qquad 0 < \eta < 1.$$

In this case, the asymptotic form of the equal-time propagator would be given by

$$G(\mathbf{p}) \propto \frac{1}{|\mathbf{p}|}\left(\frac{\Lambda_{\mathrm{QCD}}}{|\mathbf{p}|}\right)^{\eta},$$

where the divergent factor $(\Lambda_{\mathrm{UV}}/\Lambda_{\mathrm{QCD}})^{\eta}$ has been absorbed by the wave-function renormalization constant Z_3. The above picture is only one scenario which would explain the lattice data. A lattice investigation of the p_0, $\mathbf{p}$ dependence of the generalized gluon propagator $G_{ij}^{\mathrm{gen}ab}(\mathbf{p}, p_0)$ in (31) will reveal whether the above scenario applies for Coulomb gauged YM-theory. Such an investigation is left to future work.

B. Renormalization group

Perturbation theory in Coulomb gauge [34,35] is plagued by superficial divergences originating from instantaneous loops. When "supplementary rules" are introduced to define zero momentum integrals, a self-consistent framework is obtained. Within this approach, the Z_g and the ghost renormalization constants, Z_C and $Z_{\bar{C}}$, are related by [34]

$$Z_g Z_C = 1, \qquad Z_g^2 Z_C Z_{\bar{C}} = 1 - \frac{7g^2}{12\pi^2\epsilon}. \tag{48}$$

In the latter approach, dimensional regularization with the regulator $\epsilon = 4 - D$ was introduced, and an asymmetric ghost wave-function renormalization was employed yielding:

$$\widetilde{Z}_3^{-1} \equiv Z_C^{-1/2} Z_{\bar{C}}^{-1/2}.$$

We point out that our lattice results indicate that the product of bare gauge coupling g_0 and bare ghost form factor D_0, i.e., $g_0^2 D_0$, is finite, which contradicts (48). Further studies, involving simulation with larger lattices on one hand and partial resummations of perturbation theory to handle instantaneous loops on the other hand, seem necessary to resolve the above discrepancy.

VI. CONCLUSIONS

A thorough lattice study of the equal-time propagators of four dimensional SU(2) Yang-Mills theory in Coulomb gauge has been performed. Our simulations extend previous studies to larger lattices and number of different lattice spacings. Our lattice data are in good agreement with those of earlier publications [25,26,31].

We studied the transverse (equal-time) gluon propagator $G(\mathbf{p})$, the ghost form factor $d(\mathbf{p})$ and the Coulomb potential $V_{\mathrm{Coul}}(\mathbf{p})$ (20). With the help of the momentum matching technique [22], the wave functional renormalization constants are obtained for the gluon and ghost fields. In particular, we find that the combination $g_0^2 d_0(\mathbf{p})$ of the bare gauge coupling g_0 and the bare ghost form factor d_0 is renormalization group invariant.

Let us focus here on the high and the low momentum behavior. For $|\mathbf{p}| \gg 1$ GeV, our results for the (equal-time) gluon propagator show a large anomalous dimension, i.e.,

$$G(\mathbf{p}) \propto 1/|\mathbf{p}|^{1+\eta}, \qquad \eta \approx 0.5(1).$$

The high momentum behavior of the ghost form factor and of the factorization function $f(\mathbf{p})$ show the characteristic logarithmic momentum dependence, i.e.,

$$d(\mathbf{p}) \propto \ln\left(\frac{|\mathbf{p}|}{\Lambda_{\mathrm{QCD}}}\right)^{-\gamma_{go}}, \qquad \gamma_{go} = 0.26(2),$$

$$f(\mathbf{p}) \propto \ln\left(\frac{|\mathbf{p}|}{\Lambda_{\mathrm{QCD}}}\right)^{-\gamma_f}, \qquad \gamma_f = 0.47(3),$$

while a scale parameter of $\Lambda_{\mathrm{QCD}} = 0.96(5)$ GeV is consistent with the lattice data. The high momentum behavior of the Coulomb potential known from perturbation

theory [28], i.e.,

$$\mathbf{p}^2 V_{\text{Coul}}(\mathbf{p}) \approx \frac{6\pi}{11 \ln|\mathbf{p}|^2/\Lambda_{\text{QCD}}^2},$$

is recovered to high precision. The anomalous dimensions extracted from the lattice data are consistent with the sum rule $2\gamma_{go} + \gamma_f = 1$.

In the IR limit $|\mathbf{p}| \to 0$, the quantities $d(\mathbf{p})$ and $f(\mathbf{p})$ develop singularities (see also [36]). The data for the Coulomb potential are parameterized in the IR regime by

$$V_{\text{Coul}}(\mathbf{p}) \approx \frac{8\pi\sigma_{\text{coul}}}{|\mathbf{p}|^4},$$

and are consistent with linear confinement. We find that the inequality

$$\sigma_{\text{coul}} \leq \sigma$$

is satisfied. We stress that values as large as $\sigma_{\text{coul}} = (2 - $

$3)\sigma$ as reported in [25,26] are not ruled out by our data. The singularity of $V_{\text{Coul}}(\mathbf{p}) \propto 1/|\mathbf{p}|^4$, responsible for linear confinement, arises from IR singularities of the functions $d(\mathbf{p})$ and $f(\mathbf{p})$:

$$d(\mathbf{p}) \propto \frac{1}{|\mathbf{p}|^{0.49(1)}}, \qquad f(\mathbf{p}) \propto \frac{1}{|\mathbf{p}|^{1.17(10)}}.$$

The complete momentum dependence for the above functions can be found in Sec. IV.

ACKNOWLEDGMENTS

[1] J. Greensite, Prog. Part. Nucl. Phys. **51**, 1 (2003).
[2] C. D. Roberts and S. M. Schmidt, Prog. Part. Nucl. Phys. **45**, S1 (2000).
[3] R. Alkofer and L. von Smekal, Phys. Rep. **353**, 281 (2001).
[4] A. P. Szczepaniak and E. S. Swanson, Phys. Rev. D **65**, 025012 (2002).
[5] A. P. Szczepaniak, Phys. Rev. D **69**, 074031 (2004).
[6] C. Feuchter and H. Reinhardt, hep-th/0402106.
[7] D. U. Jungnickel and C. Wetterich, Prog. Theor. Phys. Suppl. **131**, 495 (1998).
[8] J. M. Pawlowski, D. F. Litim, S. Nedelko, and L. von Smekal, hep-th/0312324.
[9] V. N. Gribov, Nucl. Phys. B **139**, 1 (1978).
[10] D. Zwanziger, Nucl. Phys. B **378**, 525 (1992).
[11] H. Suman and K. Schilling, Phys. Lett. B **373**, 314 (1996).
[12] L. von Smekal, R. Alkofer, and A. Hauck, Phys. Rev. Lett. **79**, 3591 (1997).
[13] L. von Smekal, A. Hauck, and R. Alkofer, Ann. Phys. (N.Y.) **267**, 1 (1998); L. von Smekal, A. Hauck, and R. Alkofer, *ibid.* **269**, 182(E) (1998).
[14] D. Zwanziger, Phys. Rev. D **65**, 094039 (2002).
[15] J. C. R. Bloch, Phys. Rev. D **64**, 116011 (2001).
[16] C. Lerche and L. von Smekal, Phys. Rev. D **65**, 125006 (2002).
[17] C. S. Fischer and R. Alkofer, Phys. Lett. B **536**, 177 (2002).
[18] R. Alkofer, W. Detmold, C. S. Fischer, and P. Maris, Phys. Rev. D **70**, 014014 (2004).
[19] J. C. R. Bloch, Few-Body Syst. **33**, 111 (2003).
[20] A. Cucchieri, Nucl. Phys. B **508**, 353 (1997).
[21] T. D. Bakeev et al., Phys. Rev. D **69**, 074507 (2004).
[22] J. C. R. Bloch, A. Cucchieri, K. Langfeld, and T. Mendes, Nucl. Phys. B **687**, 76 (2004).
[23] J. Gattnar, K. Langfeld, and H. Reinhardt, Phys. Rev. Lett. **93**, 061601 (2004).
[24] D. Zwanziger, Phys. Rev. Lett. **90**, 102001 (2003).
[25] J. Greensite and S. Olejnik, Phys. Rev. D **67**, 094503 (2003).
[26] J. Greensite, S. Olejnik, and D. Zwanziger, Phys. Rev. D **69**, 074506 (2004).
[27] A. Cucchieri and D. Zwanziger, Nucl. Phys. (Proc. Suppl.) **119**, 727 (2003).
[28] A. Cucchieri and D. Zwanziger, Phys. Rev. D **65**, 014002 (2002).
[29] K. Langfeld, H. Reinhardt, and J. Gattnar, Nucl. Phys. B **621**, 131 (2002).
[30] D. B. Leinweber et al., Phys. Rev. D **60**, 094507 (1999); D. B. Leinweber et al., *ibid.* **61**, 079901(E) (2000).
[31] A. Cucchieri and D. Zwanziger, Phys. Rev. D **65**, 014001 (2002).
[32] C. C. Paige and M. A. Saunders, SIAM J. Numer. Anal. **12**, 617 (1975).
[33] B. Alles, D. Henty, H. Panagopoulos, C. Parrinello, C. Pittori, and D. G. Richards, Nucl. Phys. B **502**, 325 (1997).
[34] D. Zwanziger, Nucl. Phys. B **518**, 237 (1998).
[35] L. Baulieu and D. Zwanziger, Nucl. Phys. B **548**, 527 (1999).
[36] D. Zwanziger, Phys. Rev. D **67**, 105001 (2003).